Proceedings of the ASME 2010 3rd Joint US-European Fluids Engineering Summer Meeting and 8th International Conference on Nanochannels, Microchannels, and Minichannels
FEDSM-ICNMM2010
August 1-5, 2010, Montreal, Canada

FEDSM-ICNMM2010-30672

AERODYNAMIC AND THERMAL MEASUREMENTS IN A STANDING WAVE THERMOACOUSTIC REFRIGERATOR

Gaelle Poignand
LMFA UMR CNRS 5509
École Centrale de Lyon
69134 Écully cedex
France
Email: gaelle.poignand@ec-lyon.fr

Emmanuel Jondeau*
Philippe Blanc-Benon
LMFA UMR CNRS 5509
École Centrale de Lyon
69134 Écully cedex
France
Email: emmanuel.jondeau@ec-lyon.fr

ABSTRACT

Thermoacoustic refrigerators produce a cooling power from an acoustic energy. Over the last decades, these devices have been extensively studied since they are environment-friendly, robust and miniaturizable. Despite all these advantages, their commercialization is limited by their low efficiency. One reason for this limitation comes from the complex thermo-fluid process between the stack and the two heat exchangers which is still not sufficiently understood to allow for optimization. In particular, at high acoustic pressure level, vortex shedding can occur behind the stack as highlight by [Berson & al., Heat Mass Trans, 44, 10151023 (2008)]. The created vortex can affect heat transfer between the stack and the heat exchangers and thus, they can reduce the system performance.
In this work, aerodynamic and thermal measurements are both conducted in a standing wave thermoacoustic refrigerator allowing investigation of vortex influence on the system performance. The proposed device consists on a resonator operated at frequency of 200 Hz, with hot and cold heat exchangers placed at the stack extremities. The working fluid is air at ambient temperature and atmospheric pressure. The aerodynamic field behind the stack is described using high-speed Particle Image Velocimetry. This technique allows the acoustic velocity field measurement at a frequency up to 3000 Hz. Thermal measurements consist on the acquisition of both the temperature evolution along the stack and the heat fluxes extracted at the cold heat exchanger. These measurements are performed by specific micro-sensors developed by MEMS technology. The combination of these two measurements should be helpful for the further understanding of the heat transfer between the stack and the heat exchangers. .

INTRODUCTION

The thermoacoustic effect is based on the reciprocal conversion of thermal energy into acoustic energy. Classical thermoacoustic refrigerators make use of this effect which occurs inside a stack placed in a resonance tube. In such devices, the thermoacoustic process induces heat transport from one side to the other side of the stack and leads to a temperature gradient forming along the stack. The external heat transfer is then assumed by the mean of two heat exchangers placed at the stack extremities and which played a major role in the process.
Owing to their operating principle, the thermoacoustic systems offers many advantages in comparison with conventional cooling system. Among these advantages, they don't use environment harmful substances. Moreover, they are robust and miniaturizable leading to possible low cost production. From an industrial point of view, their potential application targets extend from air conditioning and heat removal from electronic components to waste heat re-use.
However, they can not yet compete with conventional cooling

*Address all correspondence to this author.

systems because of their limited efficiency arising from various losses. One important limitation in the thermoacoustic process comes from the heat exchangers. Their use for steady-flow but their methodology for heat exchangers cannot be applied in the case of an oscillating flow. Moreover, the heat transport between the stack and the heat exchangers is not sufficiently understood to enable their optimization.

Several studies have shown the existence of non-linear effects occurring close to the stack extremities [1–3]. In particular, at high acoustic pressure level, vortex shedding can occur behind the stack. In this context, numerical simulations [4–7] have shown that the created vortex can affect heat transfer between the stack and the heat exchangers and thus, decreases the system performance. In the same way, Particle Image Velocimetry (PIV) measurement techniques have been developed to characterize the turbulent flows at the end of a parallel plate stack [8, 9]. The vorticity fields behind a stack have been investigated by by Berson et al. [9], Aben et al. [10] and Shi et al. [11, 12] for different stack geometrical parameters. They categorize the vortex pattern from a single vortex pair to a vortex street depending on dimensionless parameters which are function of both stack geometry and acoustic pressure. Besides, an approximative criterion for the oscillation onset has been proposed by Berson [9]. However, in these previous studies, velocity fields are obtained by averaging instantaneous velocity fields. Such a description can be to simplistic [13], especially if the cycle-to-cycle variations of the flow field is important. These variations could have an influence on the estimation of the actual heat transfer intensity. Furthermore, the stack is not coupled with heat exchangers as it will be in a real system.

Thus, the optimisation of the heat transport in thermoacoustic systems requires to study the coupling between the stack and the two heat exchangers. For this purpose, in this work we conduct both the aerodynamic and thermal measurements in a standing wave thermoacoustic refrigerator containning a stack-heat exchangers couple. Thermal measurements consist on the acquisition of both the temperature evolution along the stack and the heat fluxes extracted at the cold and hot points of the heat exchangers. A time-resolved PIV system is used to describe the velocity field behind the stack. The advantages of these system compare to the classical PIV is the high temporal resolution which gives access to the flow time evolution. Several acoustic field can be measured during an acoustic period whereas in classical PIV, respond time is smaller than the acoustic period. Hence, this technique is better appropriate to characterize the flow behind the stack. The experimental configuration including the thermoacoustic refrigerator and the time-resolved PIV system is presented in the first paragraph. The results obtained with this configuration are presented and discussed in the second paragraph.

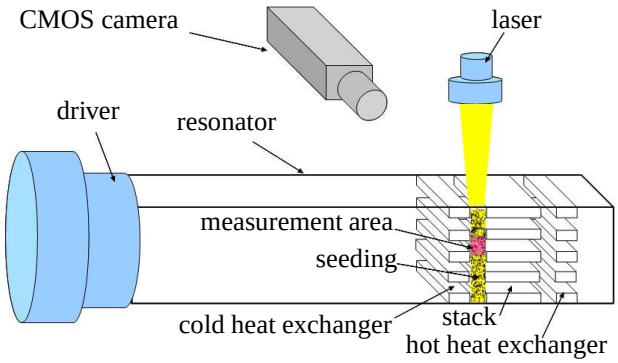

FIGURE 1. Schematic of PIV set-up.

EXPERIMENTAL SET-UP

Thermoacoustic refrigerator

The considered thermoacoustic refrigerator consists of a stack and two heat exchangers mounted inside a standing-wave resonator.

The resonator is a 86 cm length plexiglas tube with a square internal cross section of 80 $\times$ 80 cm^2. The inside working gas is air at atmospheric pressure and at room temperature. The driver is a loudspeaker (Audax HM 130 Z0) which generates a half-wavelength acoustic wave at the fundamental frequency of 200 Hz. The resonator is equipped with a 1/4¨ Brüel & Kjaer microphone flush mounted at 2 cm from the loudspeaker in order to measure the acoustic pressure. Experiments are carried out at acoustic pressure up to P_{ac} = 2000 Pa (i.e. for drive ratios up to 2%). The heat exchangers and the stack are put on a 3 cm height step to reduce their cross section area at 5 $\times$ 8 cm^2.

The stack is placed in the resonator at 76.5 cm from the loudspeaker. The stack consists of parallel glass plates. Its length is 1 cm and the spacing between two plates is 1 mm (which is five times greater than the size of thermal penetration depth in air at 200 Hz). The temperature difference ΔT between the hot and the cold stack ends is measured using two K-type thermocouples.

Thermal measurements are conducted with heat exchangers placed at a distance of 1 mm from the stack. The heat exchangers are made of parallel copper plates. These copper plates are the same thickness and spacing than the glass plates used for the stack. The plates are placed just in front of the stack plates. The ambient heat exchanger copper plates are connected at one side with a copper block in which water flows. The temperature of this block is maintained at room temperature by the circulating water. The water circulate with a flow rate of Q_w 20 ml.min^{-1}. The temperature upstream T_{win} and downstream T_{wout} of the heat exchanger are measured by thermocouples. The heat delivered to the ambient heat exchanger is obtained from $Q_h = \rho C_p (T_{wout} - T_{win}) Q_w$, with ρ the density and C_p the isobaric heat capacity per unit mass of the water.

The cold heat exchanger plates are connected to a copper plate in which a heat flux sensor is inserted. This thermal heat flux sensors have been specifically developed using MEMS technology [14]. It measures the convective heat flux exchanged between the surface on which it mounted and the environment. The output voltage of this sensor is directly proportional to the heat flux extracted Q_c to the cold heat exchanger. Its sensitivity is about 5 mV.W^{-1}.

Time-resolved PIV

Figure 1 shows the schematic of the experimental set-up. The two-dimensional instantaneous velocity field measurement are performed with a time-resolved Particle Image Velocimetry (TR-PIV) system using a high-frequency pulse laser and a high-speed camera. The TR-PIV system used is capable of acquiring 3000 PIV image frame pairs at up 3125 Hz which represents 15 velocity fields measured per acoustic period (for a frequency of 200 Hz).

The pulsed light sheet is generated by a Quantronix Darwin dual head Nd:YLF laser. The laser sheet penetrated into the resonator perpendicularly to the resonator axis and illuminated the flow in front of the stack. The nominal output pulse energy is 18 mJ/pulse/head at 3125 Hz. Air is seeded with olive oil droplets of sizes typically 1 μm. The camera used to record the light scattered by the seeded particles is a CMOS Phantom V12 camera which have 20 μm square pixels in a 1280 $\times$ 800 pixel sensor. The field of view situated behind the stack in a plane parallel to the direction of acoustic oscillations and perpendicular to the stack plates has a size of 9 $\times$ 6 mm. The recording of microphone signal is synchronised on the images recording. Simultaneous recording of the pressure level and of the velocity field permit to determine the phase ϕ between the particle velocity and the acoustic pressure and hence, to class the image versus their phase on a acoustic period. Cross correlation mode is used and the interrogation window is 16 x 16 pixels with a 50 % overlap ratio between adjacent windows.

RESULTS

In this section, the experimental results of the velocity field behind the stack without heat exchanger and the thermal behaviour of the stack coupled with the two exchangers are presented.

Figure 3 depicts the time evolution of the vorticity field during an acoustic period with a pressure of 2000 Pa. In this figure, fifteen instantaneous vorticity fields are represented. For each vorticity field, the phases ϕ between the acoustic pressure and the velocity field are indicated in the labels. The measured vortex localization and shape are not as clear as in the case of an averaged vorticity field where small-scale structure would be filtered out.

P_{ac}	u_{ac}	$2d_{ac}$	Re	St	vorticity pattern
Pa	$m.s^{-1}$	mm			
500	0.6	1.06	90	0.30	two vortices
1000	1.20	1.90	179	0.15	four vortices
1500	1.98	3.20	269	0.10	transition area
2000	2.65	4.28	359	0.07	vortex street

TABLE 1. Oscillatory flow characteristic.

The time evolution of the vorticity field can be divided into two parts. The first one, defined for a phase range increasing from 90° to 270°, is called the "ejection part": the fluid leaks out the stack. The second one, defined for a phase range decreasing from 270° to -90°, corresponds to the "suction part": the fluid gets into the stack.

At the beginning of the ejection part, the flow starts to accelerate. For ϕ=150°, the shear layers along the plates extend beyond the stack end. As a consequence, a couple of attached vortex structure is formed. The two vortices are symmetrical relatively to the plate centerline. After reaching its maximum value at ϕ=180°, the vortex shear layers outside the stack start to oscillate leading to asymmetric pairs of counter-rotating vortices formation. In the deceleration range phase going from 180° to 270°, the alternate vortex shedding becomes weaker. After the flow reversal point corresponding to ϕ= 270°, the flow slows down and gets into the stack whereas vortex structures are still present.

During an acoustic period, similar velocity field time evolutions are observed in an acoustic pressure range going from 500 Pa to 2000 Pa. However, the vortex shedding flow pattern depends on the acoustic pressure. This is clearly shown in figure 4 which represents the vorticity field for ϕ= 180° when the particle velocity is zero. For 500 Pa and 1000 Pa, two pairs of vortex structures are created. For 1500 Pa, a vortex street starts to emerge and finally, for 2000 Pa, a vortex street is formed behind the stack. To categorize the flow pattern, Aben [10] uses the ratio between the Strouhal number St and the Reynolds number Re given by:

$$Re = \frac{2y_0 u_{ac}}{\nu} \quad \text{and} \quad St = \frac{2y_0 f}{u_{ac}}, \tag{1}$$

where u_{ac} is the amplitude of the acoustic velocity inside the resonator, $2y_0$ the plate thickness and ν the kinematic viscosity of air. The different categories of vortex formation versus the ratio St/Re are indicated on the Figure 9 of [10].

These two dimensionless numbers are given for the four acoustic pressure considered in the table 1. There is a good agreement be-

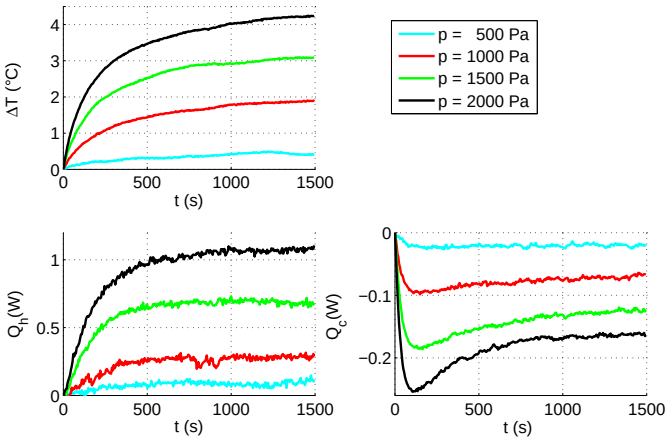

FIGURE 2. Temporal evolution of the temperature difference $DeltaT$ (a), heat flux Q_h (b) and Q_c(c) extracted and delivered to the heat exchangers for a acoustic pressure from 500 Pa to 2000 Pa .

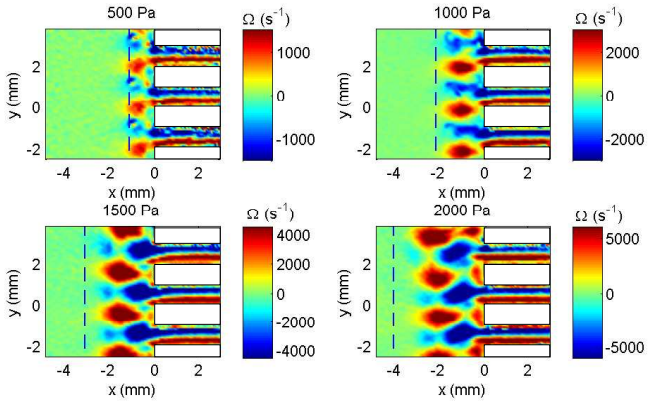

FIGURE 4. Vorticity fields for the flow at the end of the stack at 500, 1000, 1500 and 2000 Pa. The dash lines represents the distance $2d_{ac}$ from the end of the stack.

tween the flow pattern observed (which is indicated in the table 1) and the flow pattern classification determined by considering the value of the ratio St/Re.

Moreover, like noticed by Berson [15], the shear layers elongation extend about two times the acoustic displacement d_{ac} (represented by a dashed line on Figure 4). Berson [15] has also defined an empirical criterion for vortex street generation given by

$$2d_{ac} > 2y_0/0.44, \tag{2}$$

where d_{ac} is the acoustic displacement.

Here, $2y_0/0.44$ is 2.3 mm and the distance $2d_{ac}$ versus the acoustic pressure is given in the table 1. This empirical criterion is valid for an acoustic pressure above 1000 Pa which is in fair agreement with our observations.

The flow structure around the stack has been well defined here and shows vortex street generation. However, the heat transfer process influence between the stack and the heat exchangers remains undefined.

In the following, experiments are conducted with heat exchangers at the stack extremities. The heat exchangers are placed 1 mm away from the stack end. The velocity fields in this configuration are expected to be more complex than with a single stack, as it was previously observed in PIV measurements.

Figure 2 shows the evolution of the temperature difference ΔT, the heat flux Q_c extracted from the cold heat exchanger and the heat flux Q_h delivered to the ambient heat exchangers for an acoustic pressure range going from 500 Pa to 2000 Pa.

For an acoustic pressure of 2000 Pa, the temperature difference at the stack extremities reaches 4.2 °C, which is four times smaller than the theoretical one calculated using the linear steady state theory [16]. This four factor discrepancy arises from all complex thermal mechanisms which are neglected in the linear theory [17]. The heat flux Q_c is -0.250 W and the heat flux Q_h is closed to 1.1 W.

As described in the linear theory, when the acoustic pressure increases, both temperature difference ΔT, heat flux extracted (in absolute value) and delivered to the heat exchangers rise. The heat flux Q_h rejected to the environment is four times higher than the heat flux extracted at the cold side.

The time evolution of the heat flux Q_c given by the heat flux sensor shows that for a low acoustic pressure (under 500 Pa), the heat flux Q_c extracted from the cold exchanger decreases until it reaches a steady state value at 100 s after switching on the source. For higher acoustic pressure level (above 1000 Pa), the heat flux extracted at the cold exchanger quickly increases toward a maximum value at 150 s after switching on the source. From that moment on, its stabilizes and decays to a lower value. Thus, for a high acoustic pressure, the heat flux extracted from the cold heat exchanger tends toward a maximum value (in absolute value). The origin of this limitation may be the generation of vortex behind the stack which occurs for an acoustic pressure higher than 1000 Pa. This confirms our hypothesis that the formation of vortices can lead to a degradation of heat transfer between the stack and heat exchangers.

CONCLUSION

In this paper, the coupling between a stack and adjacent heat-exchangers in a thermoacoustic refrigerator is investigated. This study follows up the particle image velocimetry measurements of Berson et al. [1,9,15] in that, firstly, time-resolved particle image velocimetry is used to access to the flow time evolution

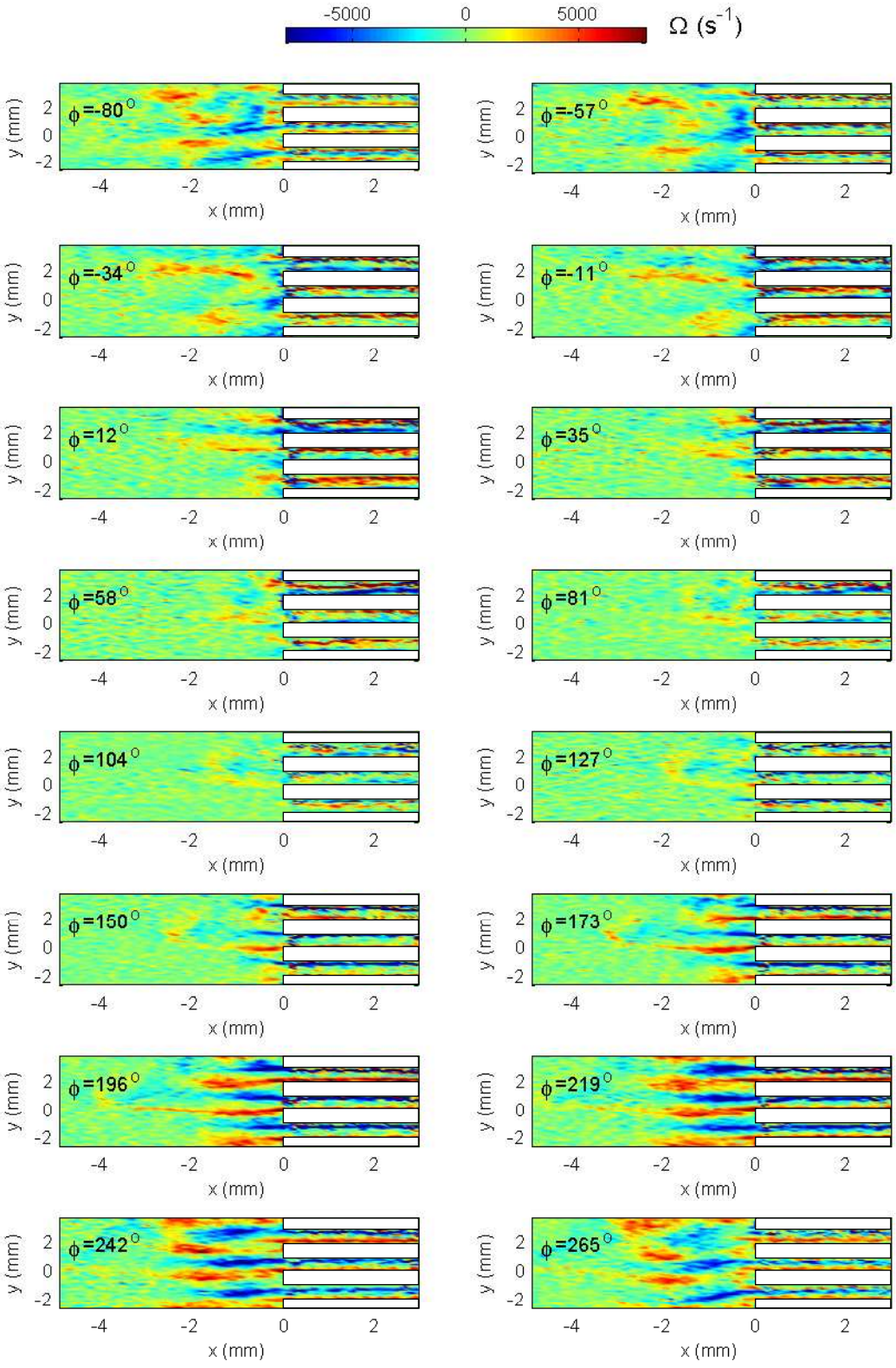

FIGURE 3. Vorticity fields for the flow at the end of the stack at 2000 Pa. The phase ϕ at which the frames are generated are indicated in the labels.

behind a single stack and secondly, these PIV measurements are completed with thermal measurements performed with the stack coupled with two heat exchangers.
PIV measurements of the flow behind a stack show that vortex shedding occurs at high drive ratios. Besides the time evolution of the heat flux extracted from the cold heat exchanger shows that the heat flux reaches a maximum (in absolute value) 150 s after switching on the source and stabilizes after at a lower level. The heat flux has a limitation which the origin may be the formation of vortices behind the stack. Experimental investigation of the velocity field with the stack coupled with some exchangers is currently in progress to valid this hypothesis. The combination of thermal and velocity field measurements is helpful for the further understanding of the heat transfer between the stack and the heat exchangers. This study is a first step and additional experiments are needed for a better knowledge of the heat transfer.

CITING REFERENCES

ACKNOWLEDGMENT

This work was supported by ANR (project MicroThermAc NT051-42101). The authors are also grateful to N. Grosjean for their assistance and the installation of the TR-PIV system.

REFERENCES

[1] Blanc-Benon, Ph., Besnoin, E. and Knio, O., 2003. "Experimental and computational visualization of the flow field in a thermoacoustic stack". *C.R. Mécanique* , **331**, pp. 17-24.

[2] Berson, A., Michard, M. and Blanc-Benon, Ph., 2007. "Measurement of acoustic velocity in the stack of a thermoacoustic refrigerator using Particle Image Velocimetry". *Heat and Mass Transfer*, **44**, pp. 1015-1023.

[3] Gusev, V., Lotton, P., Baillet, H., Job, S. and Bruneau, M., 2001. "Thermal wave harmonics generation in the hydrodynamical heat transport in thermoacoustics". *J. Acoust. Soc. Am.*, **109**, pp. 84-90.

[4] Marx, D., 2003. "Simulation numérique d'un réfrigérateur thermoacoustique". MS Thesis, Ecole Centrale de Lyon, 2003-34.

[5] Marx, D. and Blanc-Benon, Ph., 2004. "Numerical simulation of stack-heat exchangers coupling in a thermoacoustic refrigerator". *AIAA journal*, **42**(7), pp. 1338-1347.

[6] Marx, D. and Blanc-Benon, Ph., 2004. "Computation of nonlinear and edge effects in a thermoacoustic refrigerator". *7th Biennal ASME Conf. Engineering Systems Design and Analysis*, Manchester, U.K , ESDA2004-58412.

[7] Besnoin, E. and Knio O., 2004. "Numerical study of thermoacoustic heat exchangers". *Acta Acustica united with Acustica*, **90**, pp. 432-444.

[8] Mao, X., Yu, Z., Jaworski, A. J. and Marx, D., 2008. "PIV studies of coherent structures generated at the end of a stack of parallel plates in a standing wave acoustic field". *Experiments in Fluids*, **45** (5), pp. 833-846.

[9] Berson, A. and Blanc-Benon, Ph., 2007. "Nonperiodicity of the flow within the gap of a thermoacoustic couple at high amplitudes". *J. Acoust. Soc. Am.*, **122** (6), pp. EL122-EL127.

[10] Aben, P., Bloemen, P. and Zeegers, J., 2009. "2-D PIV measurements of oscillatory flow around parallel plates". *Experiments in Fluids*, **46** (4), pp. 631-641.

[11] Shi, L., Yu, Z. and Jaworski, A. J., 2009. "Vortex shedding at the end of parallel-plate thermoacoustic stack in the oscillatory flow conditions". *International Journal of Applied Science, Engineering and Technology*, **3** (5), pp. 144-151.

[12] Shi, L., Yu, Z. and Jaworski, A. J. "Vortex shedding flow patterns and their transitions in oscillatory flows past parallel-plate thermoacoustic stacks". *Experimental Thermal and Fluid Science*. DOI: 10.1016. In Press.

[13] Mao, X. and Jaworski, A. J., 2010. "Application of particle image velocimetry measurement techniques to study turbulence characteristics of oscillatory flows around parallel-plate structures in thermoacoustic devices". *Measurement Science and Technology*, **21** (3), 035403.

[14] Gaviot E., Polet F., Raucoules F., Brachelet F., Blanc-Benon Ph., "Planar Differential Radiometers. A quantitative approach to designing enhanced units", *Meas. Sci. Tech.* 10 (2), 84-92 (1999).

[15] Berson, A., 2007. "Vers la miniaturisation des rfrigrateurs thermoacoustiques : caractrisation du transport non-linaire de chaleur et des coulements secondaires", MS Thesis, Ecole Centrale de Lyon, 2007-41.

[16] Swift, G.W., 1988. "Thermoacoustic engines". *J. Acoust. Soc. Am.*, **84** (4), pp. 1145-1180.

[17] Lotton, P., Blanc-Benon, Ph., Bruneau, M., Gusev, V., Duffourd, S., Mironov, M. and Poignand, G., 2009. "Transient temperature profile inside thermoacoustic refrigerators". *International Journal of Heat and Mass Transfer*, **52** (21-22), pp. 4986-4996.